



Title	Influence of Stress-strain Curve on Post-yield Behavior of Notched Plate(WELDING MECHANICS, STRENGTH AND DESIGN)
Author(s)	Suzuki, Hiroyuki; Horikawa, Kohsuke
Citation	Transactions of JWRI. 1982, 11(1), p. 115-122
Version Type	VoR
URL	https://doi.org/10.18910/4151
rights	
Note	

The University of Osaka Institutional Knowledge Archive : OUKA

<https://ir.library.osaka-u.ac.jp/>

The University of Osaka

Influence of Stress-strain Curve on Post-yield Behavior of Notched Plate[†]

Hiroyuki SUZUKI^{**} and Kohsuke HORIKAWA^{*}

Abstract

This paper reports the study on the mechanical behaviors of notched plate and on the allowable notch size based on the elongation capacity in the two grades of steels. The tensile tests were performed on the center notched plate specimen. The elasto-plastic stress analysis was also performed to investigate on stress and strain distribution by finite element method.

The following conclusions were obtained

- 1) *The fracture mode depends on the mechanical properties and/or the stress concentration.*
- 2) *The evaluation of deformation is unavoidable as well as the strength with notched member.*
- 3) *The elongation at fracture depends on notch length and/or notch tip radius.*
- 4) *$\epsilon/\epsilon_y = 10$ is suggested for the tentative criterion for the check of deformation.*

KEY WORDS: (Stress-strain Curve) (Post-yield Behavior) (Stress Concentration) (Elongation Capacity)

1. Introduction

There are two groups of the mechanical properties of the materials, the strength such as the tensile strength and the yield point strength, and the deformation such as the elongation and the reduction of area. It is well-known that the uniform elongation decreases as the yield stress increases. This fact is recognized from experimental results on the mild steel and the high strength steel.

Structure has many stress concentrations such as bolt-hole and hand-hole. The members are usually designed that nominal stress shall be under the allowable stress even they include these stress concentrations. The influence of the stress concentration is expected to be covered by the post-yield residual strength. However, the economical design is recently required with becoming the light-weight and the large-sized structure. In addition, there is the tendency to require the elongation capacity in the structural member including the stress concentrations.^{1,2,3)}

From these reasons it is needed to clarify the post-yield mechanical behaviors of the structural member including the stress concentrations for the different mechanical properties.

There are two types of fractures; one is the load decreasing by the necking, the other is the crack initiation. Dr. Hoshino reported the analytical study on fracture of both sides U-notched tensile specimen with finite element method considering the deformation.^{4,5)} In his analysis, he defined the unstable

fracture as the state of deformation increment without load increment and the true fracture as the state when maximum plastic strain reaches the fracture strain. And they were corresponded to the load decreasing by the necking and to the crack initiation, respectively.

It is the purpose of this paper to investigate the mechanical behaviors of notched plate and the allowable notch size based on the elongation capacity. Also, it is shown that type of fracture, the unstable fracture or the true fracture, depends on the intensity of stress concentration.

2. Experiments

The center notched tensile tests on the center notched plate specimen were performed using the high strength steel of 80 kg/mm² in the tensile strength (hereinafter called HT80) and the mild steel of 41 kg/mm² in the tensile strength (hereinafter called SM41). Chemical composition and mechanical properties are shown in Table 1 and 2. Mechanical properties were obtained from coupon tests. As the yield point was not obvious in HT80, proportional limit stress was used for the yield stress. As for SM41, the yield stress was regarded as the intersecting point elastic line and plastic plateau. Gage length is 50 mm.

Test specimen configuration is shown in Fig. 1. The six kinds of center notch were used for stress concentration. Load decreasing by the crack initiation was regarded as the true fracture, and by the necking as the unstable fracture. Specimen surface was

[†] Received on March 31, 1982

^{*} Associate Professor

^{**} Research Associate

Transactions of JWRI is published by Welding Research Institute of Osaka University, Ibaraki, Osaka, Japan

Table 1 Chemical composition $\times 100(\%)$

	C	Si	Mn	P	S	Cr	Mo	V	Al	B
HT80	13	25	90	1.3	0.5	69	42	3.9	3.3	0.12
SM41	22	1	68	2.5	1.5					

Table 2 Mechanical properties

	Y.S. kg/mm ²	T.S. kg/mm ²	E1. %	Thickness mm
HT80	74.9	79.7	17.1	7.0
SM41	32.0	47.7	36.8	5.6

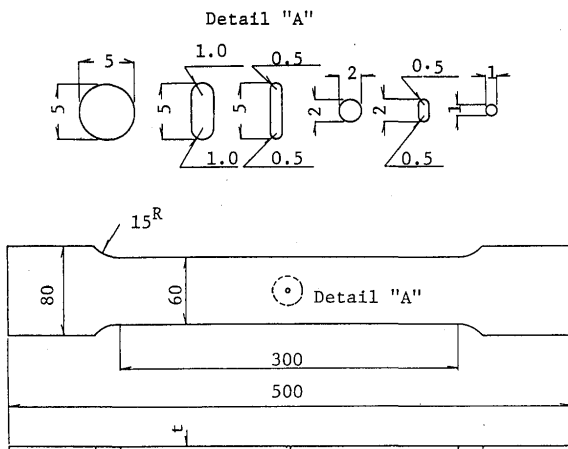


Fig. 1 Specimen configuration

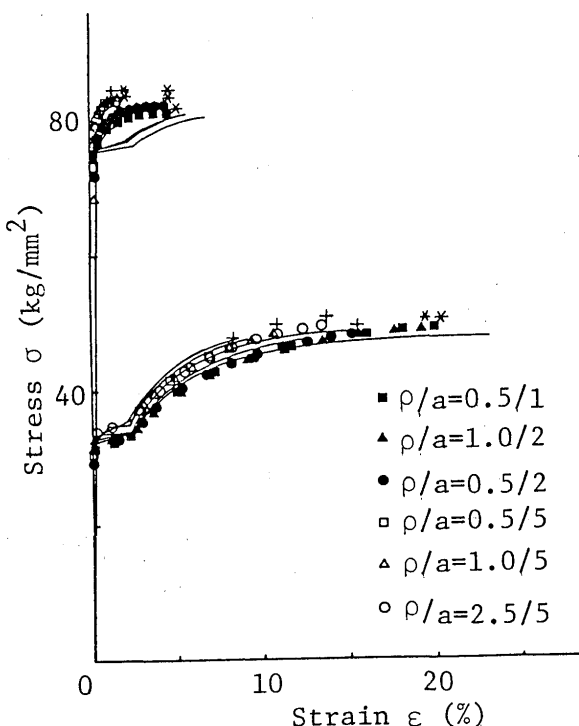


Fig. 2 Stress-strain curves (Solid lines are experimental results and symbols are analytical results. *: The unstable fracture, +: The true fracture)

polished to look for the fracture initiation by visual.

Stress-strain curves are shown by solid lines in Fig. 2. Vertical axis is the nominal stress at net section and horizontal axis is the strain of gage length=150 mm over notch. The elongation decreases remarkably according to increasing of notch length in both materials. It seems that the influence of the difference of notch tip radius on the elongation is not larger than the difference of notch length. Fracture stress at net section nearly equal to the tensile strength of coupon test, shown in Table 3. Both materials have few differences in strength regardless the ratio of notch length to specimen width, the ratio of notch tip

Table 3 Location of fracture and fracture stress

Upper line: Location of fracture

Middle line: $\frac{\sigma_{B, \text{GROSS}}}{\sigma_{B, \text{nominal}}}$

Lower line: $\frac{\sigma_{B, \text{NET}}}{\sigma_{B, \text{nominal}}}$

$\frac{a}{W}$	$\frac{\rho}{a}$	HT80	SM41
$\frac{1}{60}$	$\frac{0.5}{1}$	GROSS SECTION $\frac{78.8}{79.7} = 0.99$ $\frac{80.2}{79.7} = 1.01$	NET SECTION $\frac{46.7}{47.7} = 0.98$ $\frac{47.5}{47.7} = 1.00$
$\frac{2}{60}$	$\frac{0.5}{2}$	NET SECTION $\frac{78.1}{79.7} = 0.98$ $\frac{80.7}{79.7} = 1.01$	NET SECTION $\frac{46.0}{47.7} = 0.96$ $\frac{47.5}{47.7} = 1.00$
$\frac{5}{60}$	$\frac{1}{2}$	NET SECTION $\frac{78.4}{79.7} = 0.98$ $\frac{81.3}{79.7} = 1.02$	NET SECTION $\frac{47.0}{47.7} = 0.99$ $\frac{48.7}{47.7} = 1.02$
$\frac{5}{60}$	$\frac{0.5}{5}$	NET SECTION $\frac{73.7}{79.7} = 0.92$ $\frac{80.4}{79.7} = 1.01$	NET SECTION $\frac{42.4}{47.7} = 0.89$ $\frac{46.1}{47.7} = 0.97$
$\frac{5}{60}$	$\frac{1}{5}$	NET SECTION $\frac{72.9}{79.7} = 0.91$ $\frac{79.3}{79.7} = 0.99$	NET SECTION $\frac{43.7}{47.7} = 0.92$ $\frac{47.6}{47.7} = 1.00$
$\frac{2.5}{5}$		NET SECTION $\frac{73.8}{79.7} = 0.93$ $\frac{80.6}{79.7} = 1.01$	NET SECTION $\frac{43.4}{47.7} = 0.91$ $\frac{47.4}{47.7} = 0.99$

radius to notch length and material properties. $\sigma_{B, \text{nominal}}$ in Table 3 is the tensile strength of coupon tests, $\sigma_{B, \text{GROSS}}$ is the fracture stress for gross section and $\sigma_{B, \text{NET}}$ is for net section. Fracture modes were the crack initiation type in following specimens, the ratio of notch tip radius to notch length (hereinafter called ρ/a)=0.5/5 of HT80 and ρ/a =0.5/2, 0.5/5, 1.0/5 and 2.5/5 of SM41, and the necking type in others. Especially, ρ/a =0.5/1 of HT80 fractured at the other part of notch section by the necking. It is well-known that this is the plastic restraint.

The elongation distribution of every specimens are shown in **Fig. 3**. Vertical axis is the elongation for gage length=10 mm and horizontal axis is the location in specimen. The elongation at the other part of notch section becomes to decrease according to increasing the ratio of notch length to specimen width (hereinafter called a/W) in the same material. The elongation at the other part of notch section in $a/W=5/60$ is nearly equal to zero in HT80 having a small uniform elongation. It is clear that the total elongation of specimen was occupied by the elongation at notch section for $a=5$ mm. In general, the total elongation

of notched member depends on the quantities of the plastic deformation at the other part of notch section as shown in **Fig. 3**. HT80 has a remarkably smaller elongation than SM41 in the same notch shape. SM41 has a little difference in elongation owing to the influence of notch tip radius in the same notch length. On the other hand, HT80 has little difference. Therefore it is said that HT80 has the large strain concentration compared with SM41. And it seems that the influence of notch tip radius on the elongation of specimen is larger in SM41 than HT80.

3. Analysis

Elasto-plastic stress analysis was performed to investigate on stress and strain distribution by finite element method considering deformation. This method can easily deal with the unstable fracture and can follow the mechanical behaviors of notched member till fracture.^{5,6)} In analysis, the true fracture was defined as the state when maximum plastic strain reached the fracture strain and the unstable fracture as the state of deformation increment without load increment.

Analysis was performed on 1/4 model considering symmetry. **Figure 4** shows an example of mesh divisions; notch length=5.0 mm, notch tip radius=0.5 mm. As the constant strain element was used, the size of element at notch tip of each model was set nearly equal.

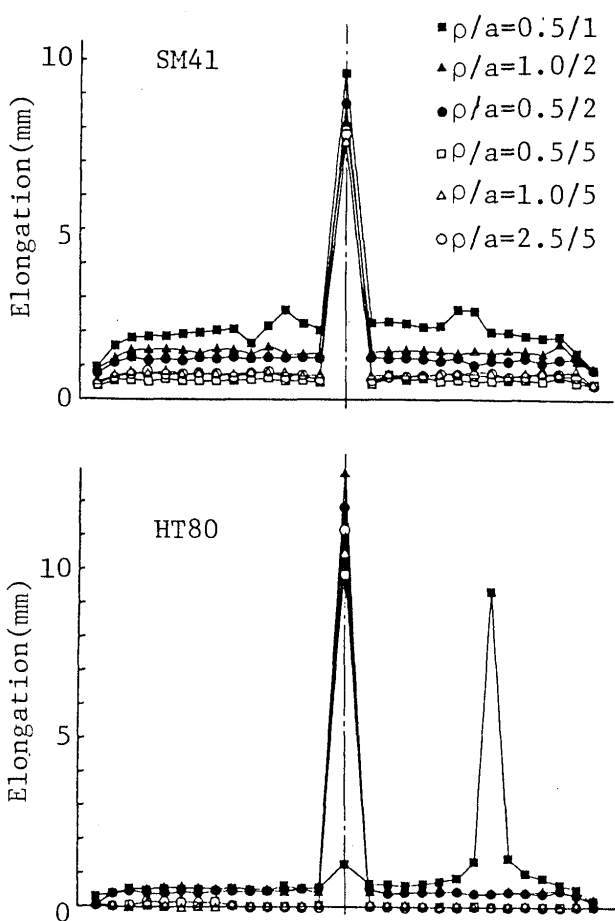


Fig. 3 Elongation distributions

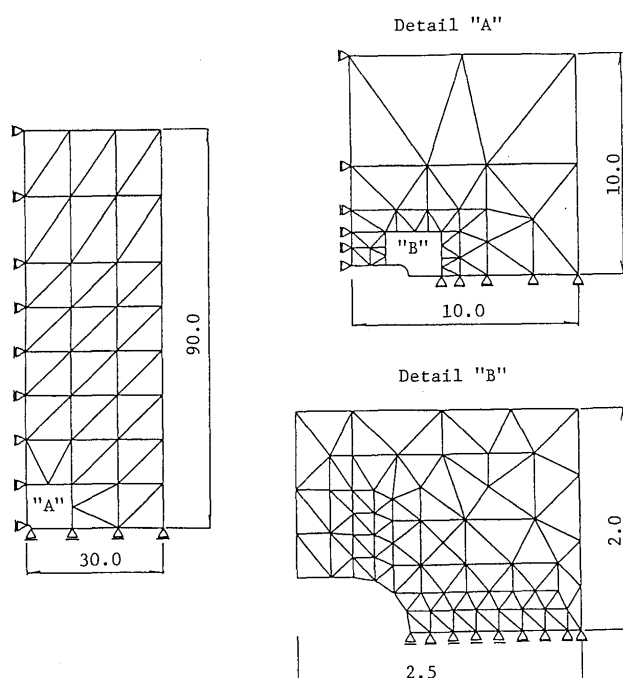


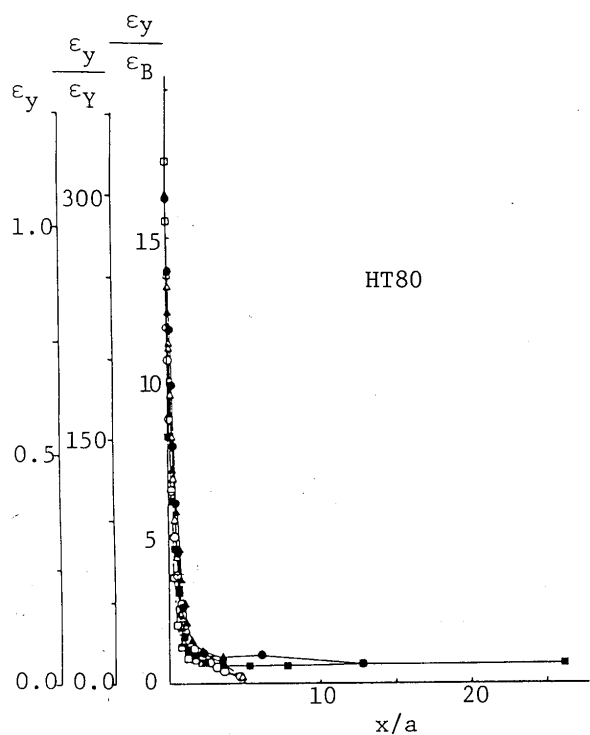
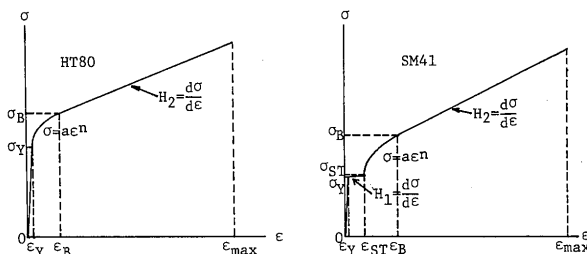
Fig. 4 An example of mesh divisions ($\rho/a=0.5/5$)

Input data are shown in **Table 4**. These were obtained from plate coupon test. However, reduction of area was measured using the round tensile specimen machined from other plate of the same grade, as it was not able to machine because of thin thickness. H_1 of SM41 is the gradient of the plastic plateau and practically equal to zero. However, H_1 was assumed as about 30 because the analytical unstable state might occur. HT80 had not the plastic plateau. In HT80 a and n were calculated from σ_y , ϵ_y , σ_B and ϵ_B , and in SM41 from σ_{ST} , ϵ_{ST} , σ_B and ϵ_B .

Stress-strain curves from analysis are shown by symbols in Fig. 2. SM41 has some scatters with strain and HT80 has a little difference with stress compared with the experimental results. It is thought that the uniform elongation supposed in analysis is less than

Table 4 Input data

	σ_y	ϵ_y	σ_{ST}	ϵ_{ST}	H_1	σ_B	ϵ_B	a	n	ϵ_{max}	H_2
HT80	74.9	0.0036	—	—	—	85.2	0.0649	96.1	0.0444	1.18	69.4
SM41	32.0	0.0015	32.5	0.0196	30.4	57.9	0.180	90.5	0.261	1.27	43.0



real value in SM41. However, they show the good agreement with the experimental results considering that analysis was performed on ideal model. Model is more rigid than experimental specimen. Experimental results include error. Fracture modes in the analysis were shown the same in the corresponding experimental results. The analysis and the experiment have a good agreement on fracture mode. Therefore the mechanical behaviors to fracture of notched plate are discussed on the results of analysis.

The distribution of true strain ϵ_y of load direction on net section at fracture is shown in **Fig. 5**. Vertical axis is true strain normalized by the true strain ϵ_B corresponding to the tensile strength. True strain of load direction and normalized one by the yield strain ϵ_y are also shown. Horizontal axis is distance from notch tip normalized by notch length a . True strain is simply called strain hereinafter. It is said from this figure that strain of load direction concentrates at notch tip in both types of fracture. Even in the specimen of $\rho/a=0.5/1$ of HT80, fractured at the other part of notch section, strain of load direction concentrates at notch tip. Strain at notch tip is about 8 times even in $\rho/a=0.5/1$ in HT80. On the other hand, in SM41 it is about 7 times for the true fracture and lower for the unstable fracture. Therefore, HT80 can endure larger strain concentration than SM41 at notch tip on the basis of ϵ_B . However, on the basis of ϵ_y SM41 can endure much larger strain concentration than

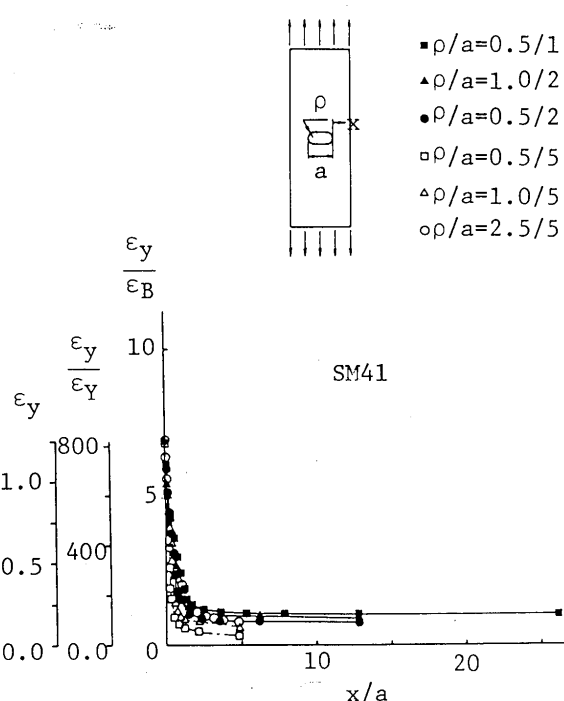


Fig. 5 Strain distributions on net section at fracture

HT80. From the point of notch shape, HT80 has little influence of notch tip radius. SM41 has the tendency that strain decreases in the far distance from notch tip according to becoming a small notch tip radius. Strain in the far distance from notch tip does not reach ε_B in HT80 because the strain ε_B differs from the work hardening exponent n in input data ($n/\varepsilon_B = 0.0444/0.0649 = 0.684$). Strain in the far distance from notch tip reaches n in $\rho/a = 0.5/1, 1.0/2$ and $0.5/2$ of HT80 and they show the elongation capacity of coupon test. Strain in the same elements reaches ε_B in $\rho/a = 0.5/1$ and $1.0/2$, and does not in $0.5/2$ of SM41. The influence of loss of area by notch is superior to the influence of stress concentration by notch shape on strain distribution in HT80 while strain distribution is subjected to both influences in SM41.

Figure 6 shows the distribution of true stress σ_y of load direction on net section at nominal yield and fracture. Vertical axis is true stress normalized by the true stress σ_B corresponding to the tensile strength. True stress of load direction and normalized one by the yield stress σ_Y are also shown. Horizontal axis is distance from notch tip normalized by notch length a . True stress is simply called stress hereinafter. The nominal yield is the state that load is equal to the product of the area of net section and the yield stress of coupon test. At the nominal yield, HT80 has the

region over σ_B at near notch tip but SM41 has not. It seems that this difference is the influence of plastic flow. The stress concentration at notch tip is remarkable in both materials according to becoming a small notch tip radius. The region over the yield stress of coupon test is nearly equal to notch length at the nominal yield. Therefore the elastic region exists in the far distance from notch tip in the models of notch length = 5.0 mm, because the region over the yield stress of coupon test is wider than others. The load at the nominal yield reaches about 90% of load at fracture in HT80 and about 60% in SM41. These values correspond to the yield ratio of each material. Therefore SM41 has a larger residual strength from the nominal yield to fracture than HT80. The residual strength seems to be independent of notch shape in this study. HT80 has little influence of notch length and notch tip radius on the stress concentration at fracture. It is thought that the stress distribution can be standardized by distance from notch tip normalized by notch length in HT80. As sharp notch has the large stress concentration at notch tip in SM41, decrease in stress in sharp notch is remarkable in the far distance from notch tip by the influence of notch shape.

As for equivalent stress $\bar{\sigma}$, though HT80 had the region over σ_B at near notch tip with almost all notch shapes in Fig. 6 at the nominal yield, equivalent stress

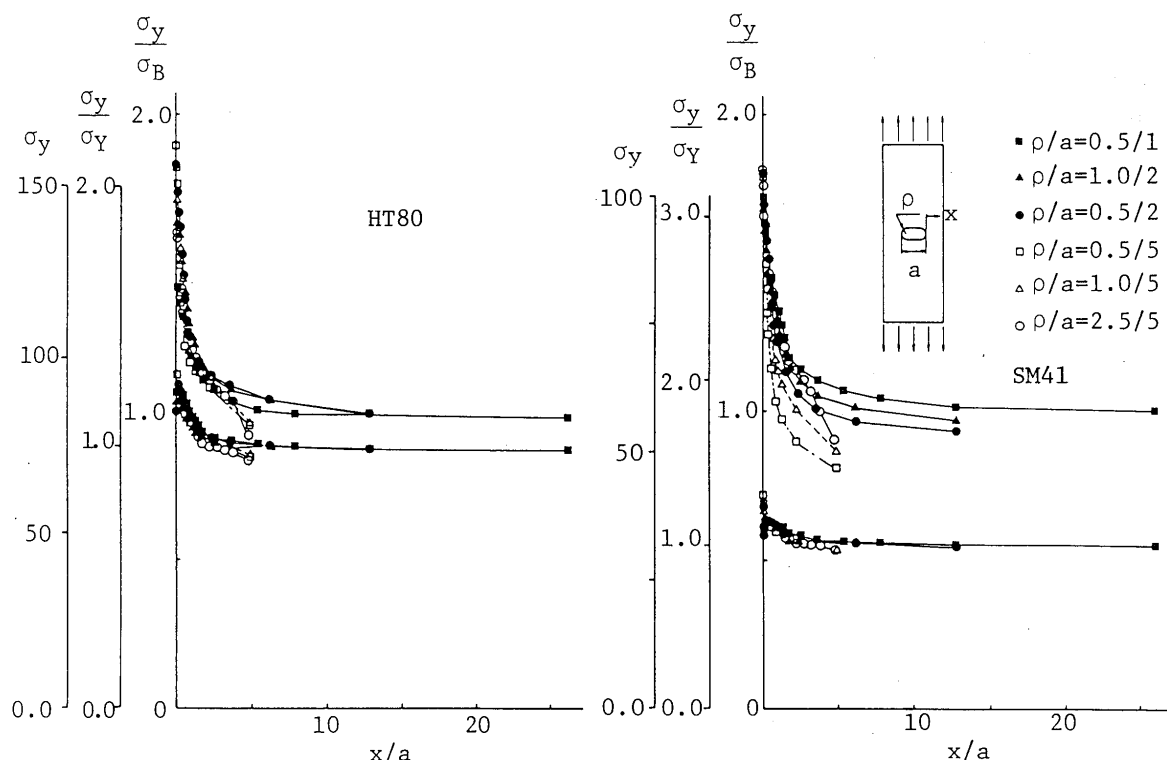


Fig. 6 Stress distributions on net section at the nominal yield and fracture

exceeded σ_B in three kinds of notch shape, $\rho/a=0.5/2$, $0.5/5$ and $1.0/5$, and their quantities were a little. In SM41, equivalent stress exceeded σ_Y at near notch tip in three kinds of notch shape, $\rho/a=0.5/2$, $0.5/5$ and $1.0/5$. Equivalent stress was nearly equal to σ_Y at the far distance from notch tip. Stress distribution at fracture had also the same tendency like at the nominal yield. It was well-known that above facts depend on the biaxial stress state and was independent of material properties and notch shape.

Stress and strain on net section were discussed to be main factor. However, the meaningful difference was not recognized between the unstable fracture and the true fracture. The distribution of stress and strain on load direction are also discussed.

Figure 7 shows the distribution of strain ϵ_y on load direction at fracture. Vertical axis is strain of load direction normalized by the strain ϵ_B corresponding to the tensile strength. Horizontal axis is distance from notch end on the center line normalized by notch width $b(=2\rho)$. This figure corresponds to Fig. 3 showing the elongation distribution. This figure shows clearly the difference caused by the effect of material properties and notch shapes. Strain ϵ_y does not reach ϵ_B in all notch shapes of HT80. As mentioned, this fact depends on the difference of ϵ_B from the work hardening exponent n in input data. The unstable fracture is analytically decided by least one of ϵ_B or n . There are the elements reaching ϵ_B (n in HT80) at the other part of notch section in $\rho/a=0.5/1$ of HT80 and $\rho/a=0.5/1$ and $1.0/2$ of SM41. It is shown from this fact that the unstable fracture may

occur at the other part of notch section in these models. Especially, the analytical results of $\rho/a=0.5/1$ of HT80 corresponds to the experimental result fractured at the other part of notch section. In HT80, strain in the far distance from notch end is nearly equal to n of coupon test without regard to notch tip radius if notch length is under 2 mm. Strain in the far distance from notch end decreases to about 15% of n without regard to notch tip radius if notch length is 5 mm. HT80 is subjected to little influence of notch tip radius. On the other hand, in SM41 strain in the far distance from notch end decreases according to smaller notch tip radius even if notch length is the same. SM41 is subjected to the influence of notch tip radius.

As the results, it is concluded that the elongation of notched member depends on the quantities of plastic deformation of the other part of notch section, the quantities of plastic deformation depend on the loss of area by the existence of notch rather than the sharpness of notch in HT80 and both factors, the loss of area and sharpness, in SM41.

The distribution of stress σ_y on load direction at the nominal yield and fracture are shown in **Fig. 8**. Vertical axis is stress of load direction normalized by the stress σ_B corresponding to the tensile strength. Stress of load direction and normalized one by the yield stress σ_Y are also shown. Horizontal axis is distance from notch end on the center line normalized by notch width $b(=2\rho)$. Stress in the far distance from notch end is nearly equal to the product of ratio of net area to gross area and the yield stress in both materials at the nominal yield. At fracture, in HT80 stress is

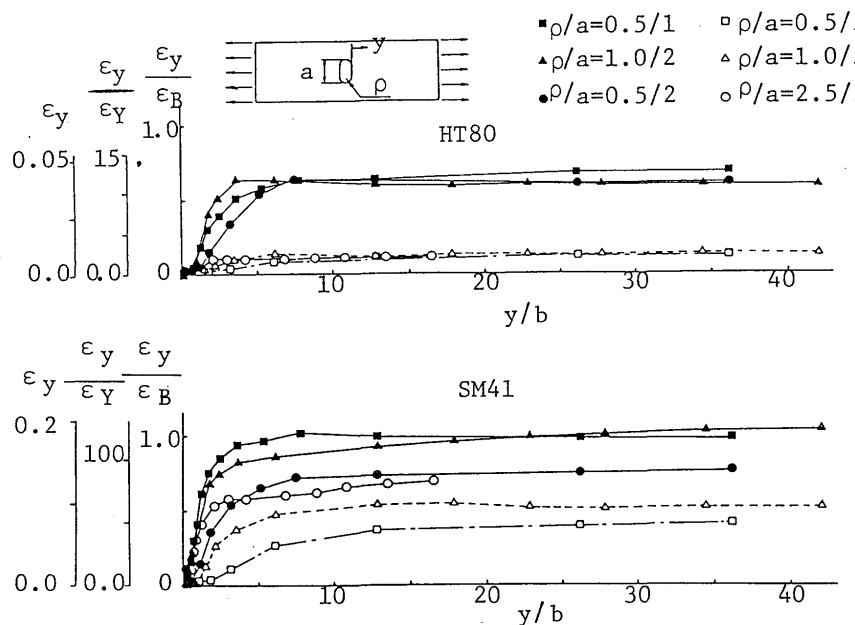


Fig. 7 Strain distributions on load direction at fracture

nearly equal to the product of ratio of area and the tensile strength. In SM41 stress does not reach the product according to smaller notch tip radius. Therefore SM41 has larger stress concentration than HT80 on the basis of above facts. Stress in the far distance from notch end is nearly equal to the yield stress in the models of notch length=5 mm of HT80. Stress in the same element is about 1.4 times of the yield stress even in $\rho/a=0.5/5$ of SM41. SM41 has a larger residual strength than HT80 on the basis of the yield stress.

As for equivalent stress $\bar{\sigma}$, equivalent stress at near notch was not equal to σ_y because of existence of σ_x . Equivalent stress became equal to σ_y to farther from notch end. The elastic region existed at near notch end in HT80 at fracture. It did not exist in SM41. Moreover, the unstable state didn't occur in analysis after all elements yielded and load increase was recognized.

It becomes clear from above results that stress and strain on load direction are subjected to the influence of notch length and/or notch tip radius. The ductility of material properties are discussed considering the elongation capacity of notched plate at fracture from the point of application to design.

The elongation capacity of notched member is very important regardless fracture mode if the plastic behaviors are considered. The ratio of slope of deflection to the yield slope of deflection, $\phi/\phi_y \doteq 10$, is considered as one of criteria on the condition in formation of plastic hinge in the plastic design.⁷⁾ The ratio of strain to the yield strain, $\varepsilon/\varepsilon_y \doteq 10$, is assumed as the criterion though load is tension in this study. Width of model is used for gage length of ε , i.e. 60 mm. Figure 9 shows correlation between $\varepsilon/\varepsilon_y$ at fracture and a/W in all models. Broken lines show the value of ε_B in HT80 and SM41 divided by ε_y and cor-

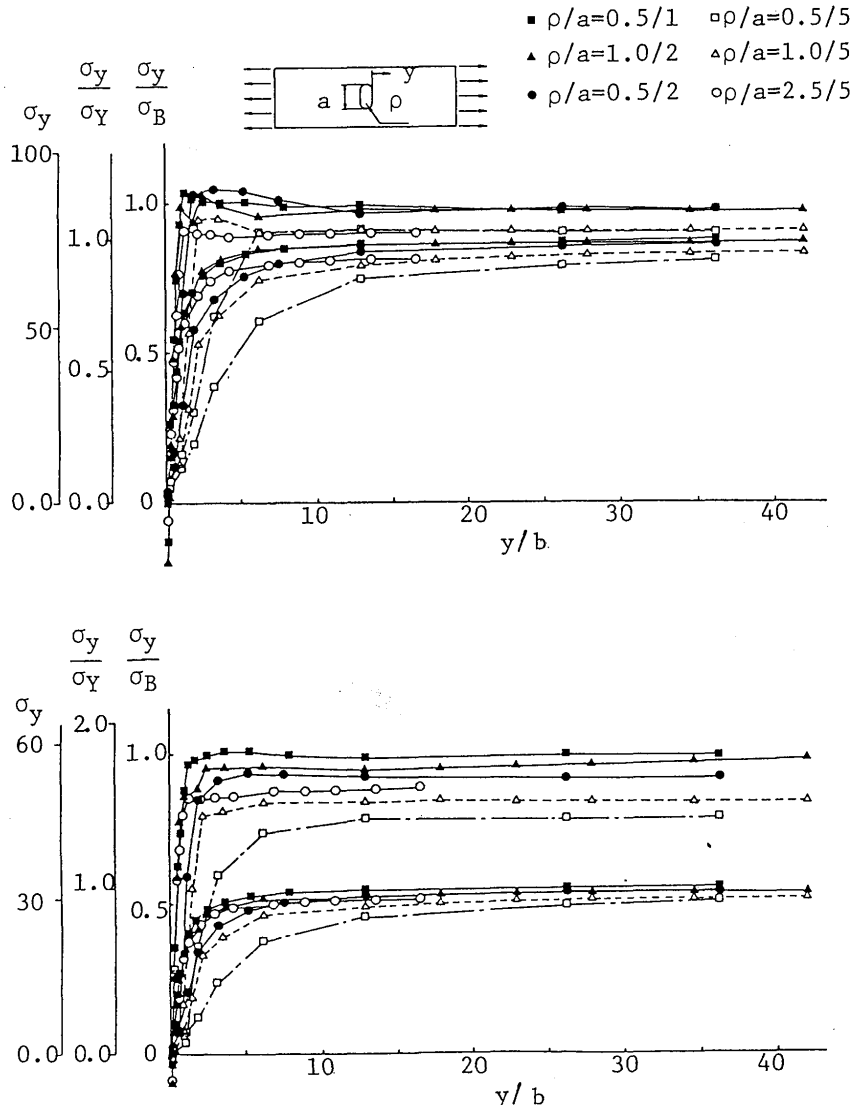


Fig. 8 Stress distributions on load direction at the nominal yield and fracture

respond to the elongation of each coupon test at fracture. Solid line shows $\epsilon/\epsilon_y = 10$. Allowable a/W is between $2/60$ and $5/60$ in HT80 on the basis of $\epsilon/\epsilon_y = 10$. The elongation at fracture is under $10\epsilon_y$ in $a/W = 5/60$ of HT80. HT80 has little influence of notch tip radius. SM41 has remarkable influence of notch length and/or notch tip radius. However, all models satisfy the criterion of $\epsilon/\epsilon_y = 10$ sufficiently in SM41.

4. Conclusions

The behaviors of center notched plate were investigated both experimentally and analytically. From this investigation, the following conclusions were obtained.

1) Whether the unstable fracture or the true fracture occurs depends on the material properties, such as the uniform elongation and the reduction of area, and the intensity of stress concentration. The unstable fracture occurs easily in the weak intensity of stress concen-

tration and the material of the small uniform elongation.

- 2) The meaningful difference was not recognized in the distribution of stress and strain on net section because of the plastic restraint. On the other hand, the meaningful difference by the notch shape was recognized on the load direction. The elongation of notched plate mainly depends on the quantities of plastic deformation at the other part of notch section and has the tendency of decreasing in accordance with longer notch length or smaller notch tip radius. Therefore the evaluation of deformation is unavoidable as well as the strength with structural member.
- 3) The elongation at fracture depends mainly on a notch length and hardly on a notch tip radius in HT80, while it depends on both of notch length and notch tip radius in SM41. The elongation decreases remarkably in accordance with smaller notch tip radius if a notch length is the same.
- 4) For the tentative criterion for the check of deformation, $\epsilon/\epsilon_y = 10$ was used. In this equation, ϵ is the strain at fracture that gage length is equal to width of specimen and ϵ_y is the yield strain. HT80 is inferior to SM41 in the elongation capacity on the basis of this criterion. The more caution must be given to notches in HT80 rather than SM41.

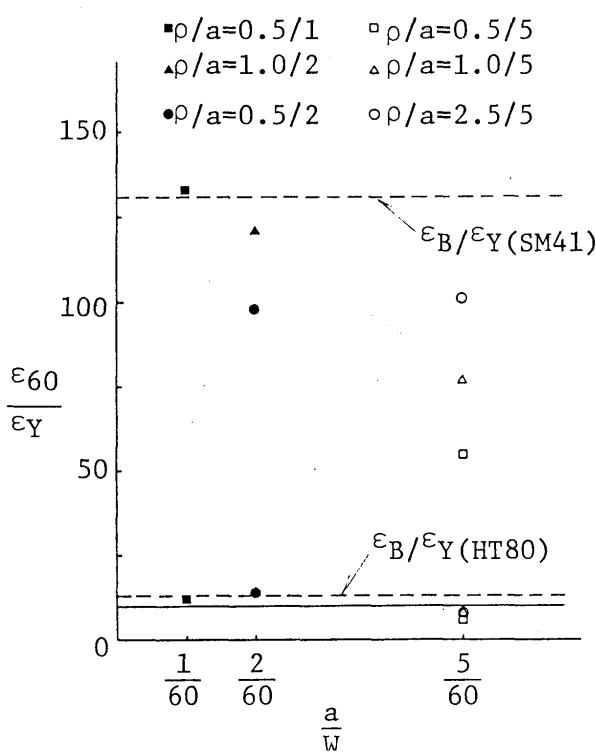


Fig. 9 Correlation between ϵ_{60}/ϵ_y and a/W

References

- 1) D. Feder and G. Werner: "Ansätze zur Traglastberechnung von Schweißverbindungen des Stahlbaus" Schweißen und Schneiden, Vol. 29, No. 4 (1977-4)
- 2) T. Suzuki and T. Ono: "Study on the plastic design of High strength steel beam" Trans. of AIJ, No. 219 (1974-5) (in Japanese)
- 3) D.R. Sherman et al.: "Ultimate Bending Capacity of Circular Tubes" Paper Number OTC 2119 (1974-5)
- 4) M. Hoshino: "Characteristics of the high strength steel as structural members" Ph. D. Dissertation, Tokyo Univ. 1970 (in Japanese)
- 5) M. Hoshino, et al.: "Elastic-plastic stress analysis on plate by finite element method considering the deformation" Sosei to kakoh Vol. 14, No. 153 (1973-10) (in Japanese)
- 6) H. Kitagawa, et al.: "Application of finite element method to large strain elastic-plastic problems and its experimental verification" Sosei to kakoh Vol. 14, No. 153 (1973-10) (in Japanese)
- 7) Y. Fujita et al.: "Plastic design" Morikita Publ. Co. 1960 (in Japanese)